Algorithmic Tunability of Quantum-Dot Infrared Detectors

Biliana Paskaleva, Unal Sakoglu, Zhipeng Wang, Majeed M. Hayat, J. Scott Tyo, and Sanjay Krishna

I. Introduction

Thanks to the recent advances in normal-incidence infrared quantum dot detectors (QDIPs), these devices are emerging as a promising technology for midwave- and long wave infrared sensing and spectral imaging. Based on intersubband transitions in nanoscale self-assembled systems, QDIPs have shown a broad spectral response that is bias dependant. While the broad spectral coverage is advantageous for broadband forward looking infrared (FLIR) imaging, it is disadvantageous for applications that require narrow spectral resolution, such as chemical agent detection. On the other hand, the bias dependant feature of the spectral response, as seen in certain QDIP devices with a dot-in-well (DWELL) structure [1], can be exploited by post-processing algorithms to achieve high levels of spectral tuning and matched filtering. As seen in Fig. 1, the detector's responsivity changes continuously in its central wavelength and shape with the applied bias voltage.

The bias-dependant nature of QDIP's responsivity is due to the quantum-confined Stark effect, which is caused by an asymmetric potential profile in the DWELL structure. For this type of QDIPs, a single detector can be operated at multiple biases sequentially, whereby the detector's responsivity changes each time the bias is varied. Therefore, a single QDIP can be exploited as different detectors; the photocurrents of a single QDIP, driven by different operational biases can be viewed as outputs of different spectrally overlapping bands. Clearly, the inherent and often significant spectral overlap in the bands of a QDIP sensor produces a high level of redundancy at the outputs of these bands. (This is not dissimilar to the redundancy present in the outputs of the cones of a human eye.) Moreover, the presence of noise in the photocurrent (i.e., dark current and Johnson noise) further complicates the process of extracting high-resolution spectral information from the highly overlapping broad spectral bands of a QDIP.

This paper presents our recent advances in post-processing techniques, developed to allow efficient utilization of QDIP's spectral responses. Our starting point is a spectral-tuning algorithm that exploits the spectral diversity in the responsivity to synthesize the output of an arbitrary target band. Then, we report a noise-modified generalization of this algorithm, based on the band-to-band signal-to-noise ratio (SNR), which has the potential for spectral tunability that accommodates and compensates the presence of noise at the output of the detector [2,3]. We show that, compared to the algorithm that does not account for the presence of noise, the noise-modified version requires significantly reduced SNR for reliable spectral tuning.

This paper also presents an optimal, problem-specific feature-selection algorithm for a general class of sensors with overlapping and noisy spectral bands. Our approach is applied to a QDIP sensor as a realistic representative of the class of sensors with overlapping bands. Comparison of the performance of the optimal features that consider the individual SNR

ELECTRICAL AND COMPUTER ENGINEERING DEPARTMENT AND CENTER FOR HIGH TECHNOLOGY MATERIALS, UNIVERSITY OF NEW MEXICO, ALBUQUERQUE, NM 87131

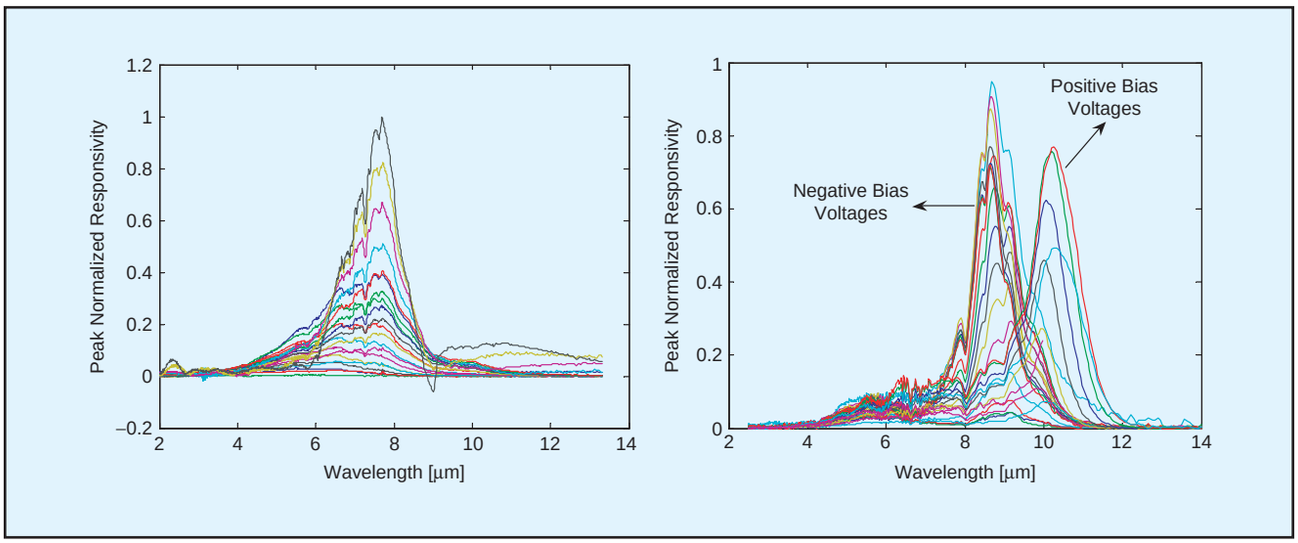

Figure 1. Spectral responsivities for QDIPs 1199 (left) and 1780 (right). The wavelength coverage for device 1199 is in the range of 4-10 μm, corresponding to bias voltages between -1 V and 1 V. The wavelength coverage for device 1780 is in the range 7-12 μm, corresponding to bias voltages in the range of -4.2 V to 2.6 V. All measurements are at detector temperature of 30K. These QDIPs were fabricated by Professor Krishna's group at the Center for High Technology Materials at the University of New Mexico.

variation and the features selected in an ideal environment, shows significant improvement in the classification results, when the noise statistics are embedded in the algorithm. The spectral-tuning and classification examples, presented in this paper, show the great potential of QDIPs as hyperspectral and multispectral sensors.

II. Geometrical Model for Spectral Sensors

In this section we review the geometrical model for spectral sensing with sensors characterized by arbitrary spectral responses as reported in [4]. The responsivity characteristics of a sensor, called spectral bands, are represented by a set of functions $\{r_i(\lambda)\}_{i=1}^{k}$. Each r_i, as a function of the observed wavelength λ, represents a set of responsivity values, see Fig. 1. The scene is described by another set of functions $\{p_i(\lambda)\}_{i=1}^{k}$, called spectral patterns. The linear space containing all these functions is termed *spectral space*, *S*. The spectral bands and pattern functions span subspaces of the spectral space, which we term the sensor *space* (*F*) and the *pattern space* (*P*), respectively.

The process of observing a pattern with a spectral sensor can be represented mathematically as an inner product between the pattern and each one of the sensor bands

$$\langle p, r_i \rangle = \int_{\lambda_{min}}^{\lambda_{max}} p(\lambda) r_i(\lambda) d\lambda = i, \qquad (1)$$

$$\langle p, r_i \rangle = \int_{\lambda_{min}}^{\lambda_{max}} p(\lambda) r_i(\lambda) d\lambda = i, \qquad (1)$$

the limits of integration in (1) are the upper and the lower bounds of the wavelength interval used for sensing. The observation produces a measurement (photocurrent) at the output of each sensor band. However, the outputs produced by a real device always include noise and cannot be represented by (1). In this case, the photocurrent at the output of band *k* can be expressed as

$$\langle p, r_i \rangle + N_i = \int_{\lambda_{min}}^{\lambda_{max}} p(\lambda) r_i(\lambda) d\lambda + N_i = \tilde{i}, \qquad (2)$$

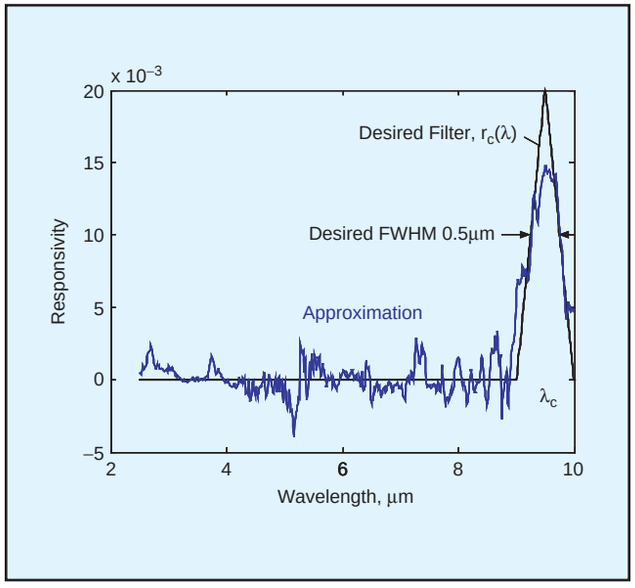

Figure 2. Linear combination, in the minimal mean-square sense, allows us to approximate desired detector response.

where N_i are independent, normally distributed random variables that represent pattern-independent noise components, see [5].

For any observed spectral pattern, the outputs corresponding to each spectral band are the *feature representations* of that pattern within the sensor space. The *spectral signature* can then be defined as the collection of the features associated with each pattern.

We define the signal to noise ratio (SNR) for the ith band of the detector as

$$SNR_i = \frac{\tilde{i}^2}{\sigma_i^2}, \qquad (3)$$

where σ_i represents the standard deviation of the noise.

III. Algorithm for Spectral Tuning

Sakouglu et al. [2,3] reported a post-processing algorithm that exploit the spectral overlap in multiple detectors in QDIPs to perform spectral sensing in the range of 3 μm-8 μm with a resolution down to 0.5 μm, which is one fourth of the spectral resolution of the detector. It has been shown theoretically in [2] that this technique is also capable of performing some level of multispectral sensing. More generally, a wide range of spectral responses, including multimodal responses, can be synthesized. Not surprisingly, the exploitation of spectral overlap in detectors to achieve high spectral resolution information is seen in the human eye, where overlapping spectral bands of cones are used to sense color.

The main idea of this algorithm can be described as follows [2]. Suppose that QDIP is operated sequentially at *k* different biases while sensing the same object, and suppose we are interested in combing the outputs of the QDIP at various biases so as to replicate the response of desired spectral filter (or band) represented by $r_c(\lambda)$. The first step of the algorithm is to form a weighted superposition of *k* QDIP responsivities to optimally approximate (in a mean-square sense) the desired band $r_c(\lambda)$, see Fig. 2. Then, by exploiting the linearity of the detector, these weights can be used to form a weighted superposition of the individual photocurrents from the detector, one for each operating bias. The resulting superposition yields the best approximation of the output of the desired spectral band $r_c(\lambda)$. Synthesized responsivities obtained in this fashion can be continuously varied, within certain limits, in shape (unimodal or multimodal), width (narrow band or wideband) and location, depending on the application requirements.

An important generalization of this post-processing algorithm, based on the band-to-band SNR, has demonstrated the potential for spectral tunability that accommodates and compensates for the presence of noise at the output of the detector, see [3]. We have applied the algorithm to QDIPs and have shown continuous spectral tuning (spectrometry) for two different source spectra, viz., a black body source with and without 3-mm polysterine filter in the range of 5-10 μm. In Fig. 3, left and right, we present the results for the case (full-width at half minimum FWHM = 0.5 and 1 μm) of reconstructing the black body spectrum for narrow and wide (FWHM = 1.5 and 2 μm) desired spectral resolutions. The performance of the algorithm was studied for both cases (once

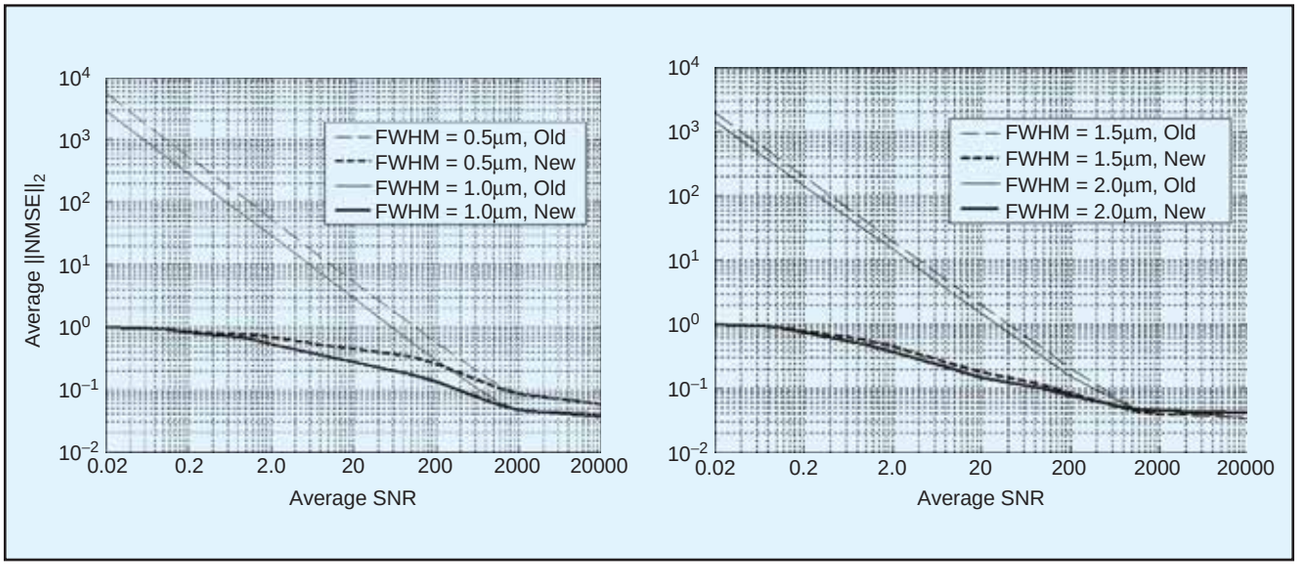

Figure 3. Comparison between original algorithm that does not accommodate noise (OLD, thin curves) and the complete algorithm (NEW, thick curves).

without considering the noise statistics and once considering the noise statistics), see [3]. As one might expect, the average normalized MSE (NRMSE) is significantly less for the noise modified algorithm compared to the old version of the algorithm. For example for an average SNR level of 2, the NRMSE is reduced by 18 dB.

We can also observe in Fig. 3 that the average NRMSE in the reconstruction decreases as the FWHM is increased, signifying the important tradeoff between the spectral resolution and robustness to the noise.

IV. Canonical Feature Selection Algorithm

1. Theoretical formulation

We can also exploit the spectral-tuning capability of a QDIP to develop a feature-selection algorithm that can be tailored to specific classification problems. More specifically, for the centers of each class of interest, we seek for the "direction" of the optimal representation of that class in the filter space. We can assume without lost of generality that the spectral bands r_i are linearly independent and form a basis in *F*. Mathematically, the best representation of p in *F* is the projection of the pattern onto the sensor space [5], which is given by the following simple equation

$$\mathrm{p}_r = \langle \mathrm{p}, \mathrm{r} \rangle \mathrm{r} = \left\langle p, \sum_i a_i \, r_i \right\rangle r = \sum_i a_i \langle \mathrm{p}, \mathrm{r}_i \rangle \mathrm{r}. \qquad (4)$$

The unit norm vector $\mathrm{r} = \sum_i a_i \, \mathrm{r}_i \in F$ gives the desired optimal direction. We term r a *superposition band* because it is in the span of the original bands r_i but is not actually one of the bands.

However, the outputs from the individual spectral bands are perturbed by noise, and different bands exhibit different noise levels (due, in the case of QDIP, to different bias voltages). As a result, the optimal superposition band is not necessarily in the direction of the projection vector. To calculate the coefficients that determine the optimal direction in the presence of noise, now must solve a constrained minimum-mean-square-error problem described as

$$\min_a E[\|\mathrm{p}_r - \mathrm{p}\|^2] = E\left[\left\|\mathrm{p} - \sum_i a_i \left(\langle \mathrm{p}, \mathrm{r}_i \rangle + N_i\right)\mathrm{r}\right\|^2\right]$$
$$\text{such that } \|\mathrm{r}\|^2 = 1 \qquad (5)$$

for the coefficients a_i. We have shown in [5] that this minimization problem is equivalent to

$$\min_a \left(1 - \cos^2 \theta_{p,r} + \sum \sum a_i \, a_j \, E[N_i \, N_j]\right), \qquad (6)$$

where $\theta_{p,r}$ is the angle between the spectral pattern p and the superposition band r.

We see from equation (6) that the contribution of a spectral band to the optimal direction depends upon two key factors: (1) the relative position of the spectral pattern with respect to that band, which is critical for reliable extraction of the relevant signal information, and (2) the presence of band-dependent additive noise at the band's output, which a results of various sensor-specific noise sources.

2. Canonical-correlation feature-selection algorithm

We now present our canonical feature-selection algorithm that determines a set of optimal directions with respect to centers of each class of interest. The algorithm utilizes the general idea from canonical correlation analysis (CCA) to measure the relationship between the sensor space *F* and the pattern space *P*. Loosely speaking, based on numerical methods for computing the principal angles θ_k between two sets of orthogonal vectors, CCA computes the canonical correlations $\sigma_k = \cos(\theta_k)$ between the two spaces spanned by these two sets of vectors. At each step *k*, σ_k is computed as $\max_{i,j} \langle \mathrm{u}_i, \mathrm{v}_j \rangle$ for every u_i in U and every v_j in V. The two vectors for which the maximum is attained are then removed from the corresponding spaces

and σ_k is defined as the smallest angle between the orthogonal compliments with respect to the remaining vectors [5].

The feature selection algorithm uses this idea to build recursively a sequence of directions that will optimally represent each pattern within the QDIP's space. The search for each subsequent optimal direction is conducted in the orthogonal complement of the previous one. The algorithm stops when one of these spaces becomes empty. The so-determined sequence of optimal directions is then used as a basis for a lower-dimensional subspace of the full sensor space.

3. Results

To evaluate the performance of the feature-selection algorithm for QDIP sensors we consider the problem of simulated rock-type classification. A comprehensive separability and classification analysis on a group of seven multispectral data sets was conducted, where each data set represents one of the seven geologically categorized rock groups [5].

We considered cases for which the average SNR of the output data assumes the values of 10, 10000 and 1000000. To enhance the separability between the classes, the optimal directions are selected with respect to the empirical means (centers) of each class. The noise statistics for the individual QDIP filters were determined after calculating the variances of a set of 100 independent measurements of the dark current for each bias voltage at a temperature of 30 K. For each average SNR, four sets of seven-band filters are defined. The first set of seven bands, termed the "noise-compensated filters," is determined by accounting for the presence of noise in the QDIP's photocurrents. The second set of seven bands, termed the "deterministic filters," is determined without considering noise in the QDIP's photocurrents. The third and fourth sets of filters respectively represent an arbitrary selection of seven QDIP bands, termed "raw-QDIP filters," and a subset of seven Multispectral Thermal Imager (MTI) bands (from 13 operational bands), which we term the "MTI filters." The four sets of filters are then applied to the training and testing data and the results of the measurements are used in a Bayesian classifier.

In Fig. 4 we show a comparison in the separability and classification performance of the noise-compensated, deterministic, raw-QDIP, and the MTI filters, all applied to noisy data. For all three SNR cases, the noise-compensated filter performs almost twice as good compared to the deterministic algorithm.

For a low SNR of 10, the error in the performance of the noise-compensated and deterministic algorithms is high; however, the performance of the noise-compensated algorithm is similar to that of MTI, showing significant improvement compared to the deterministic algorithm. The same trend follows for higher SNRs (up to 10000). The results do show, however, that the noise-compensated algorithm is more sensitive to noise compared to MTI, which is due to the high spectral overlap in the bands of the QDIP.

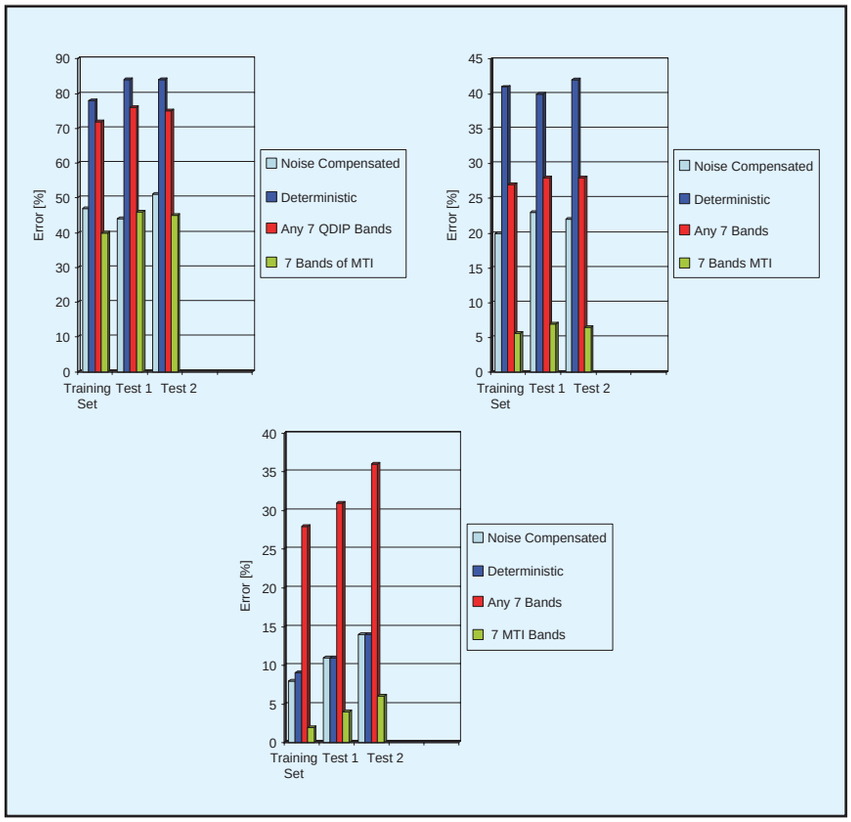

Figure 3. Comparison of the classification results for average SNRs of 10 (left), 10000 (middle) and 1000000 (right).

V. Conclusions

We reviewed spectral-tuning and feature-selection algorithms that are based on exploiting the presence of spectral overlap and bias-dependent spectral diversity in the responsivities of QDIPs. Our results suggest the potential for achieving some levels of spectral tenability and optimal feature selection by means of post-processing.

References

[1] S. Krishna, "Quantum dots-in-a-well infrared photodetectors," J. Physics D, vol. 38, pp. 2142-2150, 2005

[2] U. Sakoglu, J.S. Tyo, M. M. Hayat, S. Raghavan, and S. Krishna "Spectrally adaptive infrared photodetectors with bias tunable quantum-dots," J. Opt. Soc. Am. B, vol. 21, pp. 7-17, 2004

[3] U. Sakoglu, M. M. Hayat, J. S. Tyo, P. Dowd, S. Annamalai, K. T. Posani and S. Krishna "A statistical method for adaptive sensing using detectors with overlapping spectral band," Applied Optics, in press.

[4] Z. Wang, B. S. Paskaleva, J. S. Tyo and M. M. Hayat, "Canonical correlation analysis for assessing the performance of adaptive spectral imagers, "Proc. SPIE, vol. 5806, pp. 23-24, 2005.

[5] B. S. Paskaleva, M. M. Hayat, M. L. Martinez, Z. Wang and J. S. Tyo, "Feature selection for spectral sensors with overlapping noisy spectral bands," The SPIE Defence and Security Symposium, Algorithms and Technologies